



UNIVERSITY OF LEEDS

This is a repository copy of *Mechanical properties of rapidly solidified Ni₅Ge₃ intermetallic*.

White Rose Research Online URL for this paper:

<https://eprints.whiterose.ac.uk/122762/>

Version: Accepted Version

Proceedings Paper:

Haque, N orcid.org/0000-0002-0271-9209, Cochrane, RF and Mullis, AM (2018) Mechanical properties of rapidly solidified Ni₅Ge₃ intermetallic. In: The Minerals, Metals & Materials Society, (ed.) TMS 2018 147th Annual Meeting & Exhibition Supplemental Proceedings. TMS 2018 147th Annual Meeting of The Minerals, Metals & Materials Society, 11-15 Mar 2018, Phoenix, USA. Springer International Publishing , pp. 705-714. ISBN 978-3-319-72525-3

https://doi.org/10.1007/978-3-319-72526-0_66

(c) 2018 The Minerals, Metals & Materials Society. This is an author produced version of a paper presented at the TMS Annual Meeting 2018.

Reuse

Items deposited in White Rose Research Online are protected by copyright, with all rights reserved unless indicated otherwise. They may be downloaded and/or printed for private study, or other acts as permitted by national copyright laws. The publisher or other rights holders may allow further reproduction and re-use of the full text version. This is indicated by the licence information on the White Rose Research Online record for the item.

Takedown

If you consider content in White Rose Research Online to be in breach of UK law, please notify us by emailing eprints@whiterose.ac.uk including the URL of the record and the reason for the withdrawal request.



eprints@whiterose.ac.uk
<https://eprints.whiterose.ac.uk/>

Mechanical properties of rapidly solidified Ni₅Ge₃ intermetallic

Nafisul Haque^{1,a}, Robert F. Cochrane¹, Andrew M. Mullis¹

¹ School of Chemical & Process Engineering, University of Leeds, Leeds LS2 9JT, UK

^aCorresponding author: pmmh@leeds.ac.uk

Keywords: rapid solidification; intermetallic compound; plate & lath microstructure

Abstract

The congruently melting, single phase, intermetallic Ni₅Ge₃ has been subject to rapid solidification via drop-tube processing wherein powders with diameters between 850 – 150 μm are produced. At these cooling rates (850 – 150 μm diameter particles, 700 – 7800 K s⁻¹) the dominant solidification morphology, revealed after etching, is that of isolated plate & lath microstructure in an otherwise featureless matrix. Selected area diffraction analysis in the TEM reveals the plate & lath are a disordered variant of ε-Ni₅Ge₃, whilst the featureless matrix is the ordered variant of the same compound. Microvicker hardness test result shows that mechanical properties improve with decreasing the particle size from 850 to 150 μm as a consequence of increasing the cooling rate.

Introduction

Intermetallic compounds have been of widespread and enduring interest within Materials Science over the last 30 years or so. Such compounds are characterised by strong internal order and mixed covalent/ionic and metallic bonding, which gives rise to mechanical behaviour intermediate between ceramics and metals. A range of potential applications such as high temperature structural materials have been proposed for these materials due to good chemical stability and high hardness at elevated temperatures. However, poor room temperature ductility limits formability. Such limitations can be overcome by controlling the degree of chemical ordering present within the intermetallic, with the disordered form typically showing behaviour which is more metallic in character (higher ductility, lower hardness, and lower chemical resistance) than the fully ordered form. Rapid solidification of intermetallics is therefore an important area of study as high cooling rates are one means of suppressing ordering. Subsequent annealing of the formed part can then be utilised to restore chemical ordering, and hence the desirable properties of the intermetallic.

In this article we present an analysis of rapidly solidified Ni-37.2 at% Ge, which is close to the notional stoichiometry of the Ni₅Ge₃ compound. This is an interesting model system as, being congruently melting, the ordering reaction can be studied without any complicating solute effects. That is, we can be certain that solute partitioning, and hence also solute trapping, is absent.

The phase diagram for the Ni-Ge system has been studied extensively by Ellner et al. [1] and by Nash and Nash [2], in 1971 and 1987 respectively. More recently, further work has been also reported by Liu *et al.* [3] and by Jin *et al.* [4]. Ni₅Ge₃ is a congruently melting compound with a homogeneity range for the single phase compound of 34.6 – 44.5 at% Ge. The

congruent point is towards the Ge-deficient end of this range at 37.2 at.% Ge and 1458 K. Ni_5Ge_3 displays two equilibrium crystalline forms, ϵ and ϵ' [2] [4]. The high temperature ϵ -phase has the $P6_3/mmc$ crystal structure (Hexagonal, space group 194), while the low temperature ϵ' -phase has the C2 crystal structure (Monoclinic, space group 5) [4]. The transition between the two occurs either congruently ($\epsilon \rightarrow \epsilon'$) at 670 K for Ge-rich compositions or via the eutectoid reaction $\epsilon \rightarrow \epsilon' + \delta$ at 560 K for Ge-deficient compositions. No order-disorder transitions are shown on the phase diagram and as far as we are aware it is not known whether the high temperature ϵ phase orders direct from the liquid upon solidification or in the solid-state at some temperature below the liquidus.

Rapid solidification was affected via drop-tube processing, in which cooling rate is primarily determined by particle size. The main objective of the study is to study the mechanical properties of rapidly solidified drop-tube samples (850 – 150 μm diameter particles) with respect to increasing the rate of cooling rates.

Experimental Methods

The congruently melting ϵ - Ni_5Ge_3 compound exists over the homogeneity range of 33.8 to 43.2 at. % Ge [5]. Single phase ϵ - Ni_5Ge_3 was produced by arc-melting Ni & Ge together under a protective Ar atmosphere. To ensure homogeneity of the final alloy, the arc-melting process was repeating 8 times with the phase composition of the subsequent ingot being confirmed by XRD using a PANalytical Xpert Pro. Only when the material was confirmed as single phase was rapid solidification processing undertaken.

Rapid solidification was affected by drop-tube processing using a 6.5 m drop-tube. The tube was rough pumped to a pressure of 2×10^{-4} Pa before being flushed with N_2 gas. The rough pump – flush cycle was repeated three times before the tube was evacuated to a pressure of 4×10^{-7} Pa using a turbo-molecular pump. For sample processing the tube was filled with dried, oxygen free N_2 gas at a pressure of 50 kPa. The alloy sample, of approximately 9.4 g mass was loaded into an alumina crucible which has three 300 μm laser drilled holes in the base. Induction heating of a graphite subsector was used for heating the sample. Temperature determination was by means of an R-type thermocouple which sits inside the melt crucible, just above the level of the melt. When the temperature in the crucible attained 1533 K (75 K superheat) the melt was ejected by pressuring the crucible with ~ 400 kPa of N_2 gas. This produces a fine spray of droplets which subsequently solidify in-flight and are collected at the base of the tube.

The sample was weighed following removal from the drop-tube and sieved into the size fractions ranges from 850 μm (700 K s^{-1}) to 150 μm (7800 K s^{-1}). For each size fraction the cooling rate, calculated using the methodology described in [6], is shown in brackets.

All of drop-tube powders were subject to XRD analysis to ensure they remained single-phase prior to further analysis. Each sieve fraction was then mounted in transoptic resin and prepared for microstructural analysis using OM (Olympus BX51) and SEM (Carl Zeiss EVO MA15 scanning electron microscope). For such analysis samples were etched for 25 seconds in a mixture of equal parts of undiluted $\text{HNO}_3 + \text{HCl} + \text{HF}$. An Oxford Instrument X-Max Energy-Dispersive X-Ray (EDX) detector was used to check the chemical homogeneity of the etched samples. Bright-field imaging and selected area diffraction analysis in the

transmission electron microscopy (TEM), using an FEI Tecnai TF20, was used to distinguish between the ordered and disordered variants of each morphology observed. Samples were prepared for TEM analysis using a FEI Nova 200 Nanolab focused ion beam (FIB), with the sections cut being approximately $10\ \mu\text{m} \times 7\ \mu\text{m}$ and between 55-70 nm in thickness. An example of a FIB milled section for the related $\beta\text{-Ni}_3\text{Ge}$ compound is shown in [7]. For measurement of micro-hardness of the drop-tube samples a TUKONTM 1202 Wilson Hardness (micro-Vickers) test rig was used with 0.05 kg load. The final measurement of hardness for each sample was based upon an average of at least 10 individual measurements.

Results & Discussion

In drop-tube processing the cooling rate is determined primarily by the ratio of surface area to volume of the droplet, giving a one-to-one relationship between droplet diameter and cooling rate. Therefore a spray with a broad size distribution is used to access a wide range of cooling rates within a single experiment. The process describe in [6] equates the radiative and convective heat flux through the droplet surface with the total heat loss to obtain the cooling rate. However, we make one modification to the method given in [6]. As order/disorder reactions occur in the solid-state, the cooling rates quoted here are given immediately post-solidification, i.e. the effect of latent heat is ignored. The cooling rates for each size fraction are: $850\ \mu\text{m}$ ($700\ \text{K s}^{-1}$), $500\ \mu\text{m}$ ($1400\ \text{K s}^{-1}$), $300\ \mu\text{m}$ ($2800\ \text{K s}^{-1}$), $212\ \mu\text{m}$ ($4600\ \text{K s}^{-1}$) and $150\ \mu\text{m}$ ($7800\ \text{K s}^{-1}$).

The starting material for the drop-tube experiments was single phase $\varepsilon\text{-Ni}_5\text{Ge}_3$, which was confirmed by XRD analysis on a polished surface of the arc-melted ingot. The XRD peaks in Figure 1 clearly indicate that $\varepsilon\text{-Ni}_5\text{Ge}_3$ is the only phase present (for reference, the ICCD reference pattern 04-004-7264 for $\varepsilon\text{-Ni}_5\text{Ge}_3$ is shown on the x-axis). XRD analysis was also conducted on each size fraction of the drop tube powders and again each was confirmed as containing only $\varepsilon\text{-Ni}_5\text{Ge}_3$. For the sake of brevity, only one example result of this is shown in Figure 1, that for the 500 – 300 μm size fraction.

Figure 2 (a) shows a SEM micrograph of a polished and HF etched sample of sieve fraction 500 – 300 μm in powder form, wherein numerous plate & lath like structures are evident in the sample. Such structure are also observed in the other size fractions considered in this paper. Such structures are common in intermetallic compounds [8-10] and some alloys of iron [10]. A study conducted by Hyman *et al.* [8] observed that the formation of these lath and plate structure in $\gamma\text{-TiAl}$ during the transformation in the solid state of α dendrites during cooling to $\alpha_2 + \gamma$ mixture lath which is surrounded by γ segregates. McCullough *et al.* also observed that $\alpha_2\text{-Ti}_3\text{Al}$ also shows plate and lath morphology which is like $\varepsilon\text{-Ni}_5\text{Ge}_3$, shares the P63/mmc space group [9].

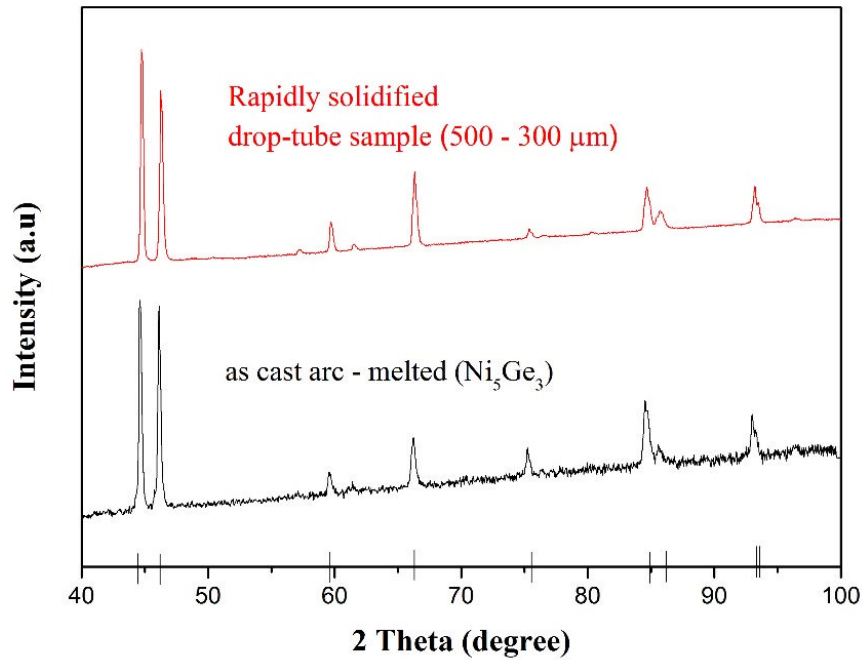


Figure 1: X-ray diffraction analysis of an arc melted sample prior to drop-tube process (black) and the rapidly solidified drop-tube processed sample 500 – 300 μm size fraction. Vertical black lines indicate peak position for the ε-Ni₅Ge₃ reference pattern.

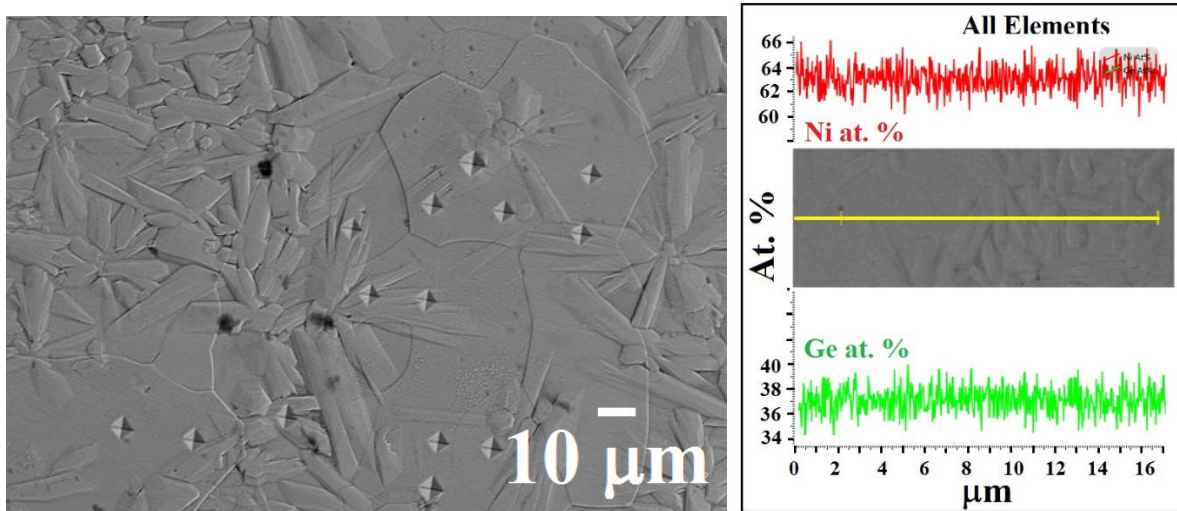


Figure 2: (a) SEM micrograph of HF etched ε-Ni₅Ge₃ drop-tube particle from the 500 – 300 μm size fraction showing plate & lath structures in a featureless matrix and (b) EDX line scan across a plate & lath trunk showing that the contrast revealed by etching is not the result of solute partitioning.

The contrast between the surrounding matrix material and the plate & lath is interesting in that, as confirmed by XRD analysis, it is not the result of contrast between different phases, the material here being single phase ε-Ni₅Ge₃. An EDX line scan perpendicular to a plate & lath is shown in Figure 2 (b). This shows that the material is chemically homogeneous and that the contrast is therefore not the result of compositional difference between the plate & lath and the surrounding matrix, as might arise from solute partitioning during solidification

[11, 12]. We conclude therefore that the contrast revealed by etching does not indicate any relation to phase difference (XRD) nor chemical composition (EDX).

In order to understand the origin of plate & lath morphologies revealed by etching in the rapidly solidified Ni_5Ge_3 drop-tube samples, TEM imaging and Selected Area Diffraction (SAD) analysis has been performed. Figure 3(a) shows a TEM bright field image of an FIB section of a lath and plate structure and some of the immediately its surrounding matrix material. Selective area diffraction (SAD) identifies two region Figure (a); (i) matrix material that is away from plate and lath structure, and (ii) inside the plate and lath structure. The SAD results of region (i) and (ii) are shown in Figure 3 (b-c) respectively. Supper lattice spots are clearly visible in Figure 3b indicating the matrix material is the chemically ordered structure. On the other hand, the absence of supper lattice spot in Figure 3c suggest the plate and lath morphology is composed of the chemically disordered material. We conclude that the contrast displayed by etching is because of incomplete chemical ordering, causing the etchant to attack the disordered material and leaving the ordered material unaffected. The lower chemical resistance of the disordered phase has resulted in this type of differential etching between ordered and disordered material to be observed previously in other intermetallic compounds [11, 13].

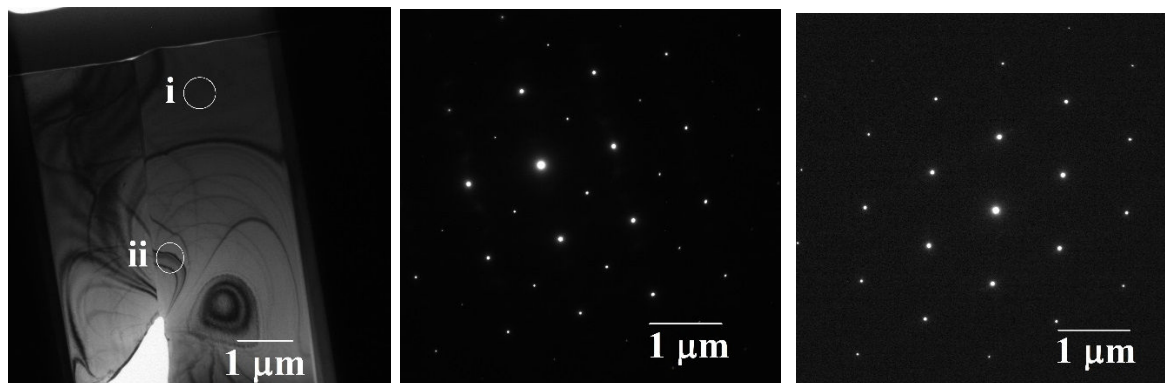


Figure 3: (a) TEM bright field image of a plate & lath structure and surrounding matrix material in a 500 – 300 μm size fraction, (b and c) selected area diffraction patterns from regions (i) and (ii) identified in the bright field image (i) matrix materials well away from the plate & lath structure, (ii) inside the structure.

In order to determine the effect of cooling rate upon mechanical properties, microvicker hardness tests have performed on the plate & lath microstructure contained within all of the sample sizes considered here (850 – 150 μm). The results of this are shown in the Figure 4. The maximum hardness, 824 Hv0.05, was observed in smallest size drop-tube sample (212 – 150 μm diameter particles). Conversely, the minimum hardness was observed in largest drop-tube sample (850 – 500 μm diameter particles). It can be concluded that the mechanical properties can be altered (hardness increased) by increasing the cooling rate, in the cases studied here from 700 to 7800 Ks^{-1} .

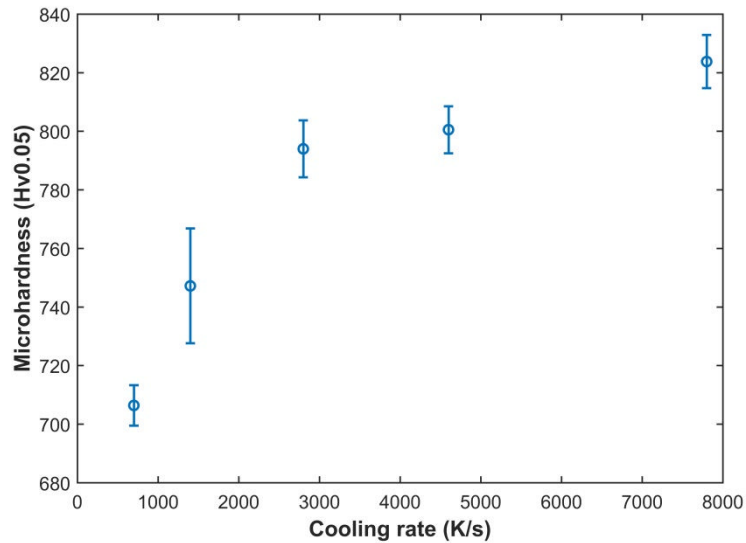


Figure 4: Micro-hardness value (in Hv0.05) as a function of droplet diameter ranges from 850 – 150 μm .

The behavior observed here is anomalous and quite contrary to what we would predict. We presume that the plate and lath structures are partially ordered while the matrix material is (near) fully ordered, this being consistent with the TEM results. However, we must suppose that with increasing cooling rate chemical ordering will be suppressed and that consequently the degree of ordering within the partially ordered material will decrease (i.e. the plate and lath structures will become more disordered with increasing cooling rate. However, we would expect that this would cause the microhardness to decrease with increasing cooling rate rather than to increase, as the disordered material because more metallic like with increasing degree of disorder. Many materials will show an increase in strength with rapid solidification due to the Hall-Petch effect, although this does not appear likely here where we are considering microhardness measurements on individual ordered and disordered regions within grains. A possible explanation would be that there is an increase in defect concentration within the lattice due to increased growth velocity at high cooling rate. This may lead to an increase in dislocation density, giving a work-hardening like effect. As such, these results may have significant implications for our understanding of the way in which rapid solidification can be used for the processing of intermetallic materials.

Acknowledgments

Nafisul Haque is thankful to the Higher Education Commission (HEC) Pakistan and NED University of Engineering & Technology for financial support.

References

- [1] M. Ellner, T. Gödecke, K. Schubert, Zur struktur der mischung Nickel-Germanium, *Journal of the Less Common Metals*, 24 (1971) 23-40.
- [2] A. Nash, P. Nash, The Ge– Ni (Germanium-Nickel) system, *Journal of Phase Equilibria*, 8 (1987) 255-264.
- [3] Y. Liu, D. Ma, Y. Du, Thermodynamic modeling of the germanium–nickel system, *Journal of Alloys and Compounds*, 491 (2010) 63-71.

- [4] S. Jin, C. Leinenbach, J. Wang, L.I. Duarte, S. Delsante, G. Borzone, A. Scott, A. Watson, Thermodynamic study and re-assessment of the Ge-Ni system, *Calphad*, 38 (2012) 23-34.
- [5] A. Nash, P. Nash, Binary Alloy Phase Diagrams, in: US National Bureau of Standards Monograph Series 25, Elsevier, ASM, Ohio, 1976, pp. 35.
- [6] N. Haque, R.F. Cochrane, A.M. Mullis, The Role of Recrystallization in Spontaneous Grain Refinement of Rapidly Solidified Ni₃Ge, *Metallurgical and Materials Transactions A*, 1-8.
- [7] N. Haque, R.F. Cochrane, A.M. Mullis, Rapid solidification morphologies in Ni₃Ge: Spherulites, dendrites and dense-branched fractal structures, *Intermetallics*, 76 (2016) 70-77.
- [8] M. Hyman, C. McCullough, J. Valencia, C. Levi, R. Mehrabian, Microstructure evolution in TiAl alloys with B additions: conventional solidification, *Metallurgical Transactions A*, 20 (1989) 1847.
- [9] C. McCullough, J. Valencia, C. Levi, R. Mehrabian, Microstructural analysis of rapidly solidified Ti□ Al□ X powders, *Materials Science and Engineering: A*, 124 (1990) 83-101.
- [10] T. Broderick, A. Jackson, H. Jones, F. Froes, The effect of cooling conditions on the microstructure of rapidly solidified Ti-6Al-4V, *Metallurgical Transactions A*, 16 (1985) 1951-1959.
- [11] N. Haque, R.F. Cochrane, A.M. Mullis, Disorder-order morphologies in drop-tube processed Ni₃Ge: Dendritic and seaweed growth, *Journal of Alloys and Compounds*, (2016).
- [12] N. Haque, R.F. Cochrane, A.M. Mullis, Morphology of Order-Disorder Structures in Rapidly Solidified L12 Intermetallics, in: TMS 2017 146th Annual Meeting & Exhibition Supplemental Proceedings, Springer, 2017, pp. 729-736.
- [13] N. Haque, R.F. Cochrane, A.M. Mullis, Morphology of Spherulites in Rapidly Solidified Ni₃Ge Droplets, *Crystals*, 7 (2017) 100.